A modular Gravity-Driven Ultrafiltration (GDU) membrane system for contaminant removal: Dynamic flux modelling and its fouling study

Boon Seng Ooi (chobs@usm.my)
Universiti Sains Malaysia
Nur Ir Imani Ishak
Universiti Sains Malaysia
Derek Chan Juinn Chieh
Universiti Sains Malaysia

Research Article

Keywords: water membrane treatment, gravity-driven membrane filtration, ultrafiltration, hollow fibre membranes

Posted Date: February 2nd, 2022

DOI: https://doi.org/10.21203/rs.3.rs-1245660/v1

Abstract

During flood or drought, water shortage is a critical issue due to the water contamination. Under this situation, gravitational driven ultrafiltration (GDU) membrane system which solely depends on hydrostatic pressure could be employed to provide the clean water for domestic usage. Due to the limitation of site accessibility during flood, a modular and batch type GDU membrane system is required for water filtration. In that case, prediction of the water level within the module which affected the hydrostatic pressure and effective filtration area over the time is important. The prediction of water level enables the design of the intermittent pumping frequencies for the optimum usage of energy. In this work, the removal efficiency of GDU system towards two common contaminants in water surface namely humic acid and calcium carbonate were tested. The highest removal efficiency of the GDU system towards humic acid, and calcium carbonate were recorded as 94.96 % and 99.19 % respectively. It was found that different feed solutions exhibited different fluxes declination profiles due to their distinctive fouling characteristic. A model was developed to predict the ideal dynamic flux of the membrane under the condition of reducing hydrostatic pressure and effective membrane area. Using the dynamic model, the resistance of the membrane and cake layer were determined. It was found that the filtration resistance is dominated by the cake layer resistance. River water test showed that GDU is an effective method for reclaiming the river water in removing the colour and turbidity.

Introduction

The weather in Malaysia is hot and humid throughout the year. Some region in Malaysia especially the state in the East Coast hit by heavy Monsoon rain annually. During the monsoon seasons, heavy rainfall might cause disastrous floods and landslides. Potable water during flood especially for the remote area are essential to maintain the basic operation of life. The consumption of water and population growth are substantially increased due to the demands of global freshwater resources and the threat of scarcity and insufficient water reservoir. Just about two-thirds of the universal population has been estimated facing the problem of water shortage for the past respective years (Mekonnen & Hoekstra 2016). Membrane separation is a common process for water treatment that provide an absolute barrier for microbes, turbidity and colour. However, pressure driven membrane process requires electricity to provide the trans-membrane pressure which might be unavailable for the remote area or during flood. Alternatively, gravitational driven ultrafiltration (GDU) membrane can be designed for filtration system to operate based on hydrostatic pressure or gravitational force.

Gravity-driven ultrafiltration (GDU) membrane system has wide application for water or wastewater treatment that has low osmotic pressure and dilutive nature. However, it also shows promising application in seawater pretreatment (Peter-Varbanets et al. 2010). Due to its simplicity operation, GDU membrane systems are notably suitable for portable or remote area of developing countries and in case of disaster (Tobias & Bérubé 2020). GDU membrane is a self-sustained process whereby an ultra-low permeate flux can be maintained by providing a relatively low hydrostatic pressure as the driving force for permeation. Recently, GDU membrane system has shown a significant capability as an extremely low-

energy for surface water treatment process caused by a driving force of water gravity (40 – 100 cm) (Pronk et al. 2019). Previous researchers have stated that the GDU membrane systems have responsibility over extended periods in drinking water treatment applications. However, there is no mitigation of fouling condition including backwash, chemical cleaning, aeration was reported in order to achieve relatively stable flux.

In one of the lab-scale tests, stabilized flux within the range of 2-20 L/m^2hr was achieved for GDU system without the need of back-washing (Derlon et al. 2016; Derlon et al. 2013; Derlon et al. 2012). GDU process consumes less energy compared to conventional ultrafiltration (UF) pretreatment (Akhondi et al. 2015), however it is also suffered from low permeate flux than that of conventional pressure-driven membrane system (Xu et al. 2021). According to Ding *et al.* the application of the GDU membrane process in treating rainwater works effectively for the removal of colloids and bacteria. However, due to the low rejection of low MW humic-like species, the system was ineffective in NOM removal (Ding et al. 2017). Commonly, GDU is operated in a dead-end mode without any pretreatment, flushing or cleaning. In one of the studies, natural water (river, spring, well or rainwater) were used as feed to the GDU system without pre- or post-treatment. The flux was stable around 4-10 L/m^2hr at hydrostatic pressure of 65 mbar and operated for 2 years (Peter-Varbanets et al. 2011). GDU filtration has been considered as a viable alternative in both wastewater and water treatment due to its low energy requirement (Wang et al. 2017).

Under the adverse flooding conditions, a modular GDU operated under batch mode is required due to the system transportation issue. For a small-scale system or under the condition that transportation of tank system is difficult, source water which fed in a batch mode faces the issues of depleting hydrostatic pressure and reducing effective area over the time. On the other hand, for system with pumping availability, the intermittent pumping could save up the energy cost by allowing the depleting water level or hydrostatic pressure. Another problem associated with the GDU system is the fouling problem due to the absence of scouring effect. For application of UF and MF system in surface water treatment, fouling via pore blocking or cake layer deposition are common especially when the water consists of extracellular polymeric and humic substance (Meng et al. 2009). At the initial stage of filtration, pore blocking was the dominating fouling mechanism followed by the steady cake layer formation under long operation time. For instance, Peter-Varbanets et al. found that the stable flux could be achieved after the complete deposition of biofoulants (Peter-Varbanets et al. 2012; Peter-Varbanets et al. 2011).

The fouling characteristic is governed by both physical and chemical interactions between the foulants constituents and the membrane surface. It is extensively believed that the water selectivity and permeability of the GDU membrane process are eminently depending on the criteria of fouling layer on the membrane surface (Derlon et al. 2012; Wang et al. 2018). The heterogenous fouling layer will provide salubrious condition to inhabited microorganisms (Zhang et al. 2018), and also encouraging the degradation of natural organic matters (NOMs) and biological macromolecules. For instance, protein, polysaccharide, humic acid, fulvic acid and many more (Chomiak et al. 2015; Derlon et al. 2013; Kohler et al. 2014). GDU membrane also applied to treat ground water with the presence of Mn^{2+}, it was found that the Mn^{2+} removal was mainly contributed by the biocake layer rather than UF membrane itself (Tang et

al. 2021). The presence of Mn^{2+} facilitated the formation of heterogeneous structures of biocake layer to primarily determine the flux stabilization of GDU membrane, while the influence of extracellular polymeric substances (EPS) concentrations was nearly negligible. Recent studies outlined the various factors of membrane fouling which included the characteristic of the foulant (composition and concentration), solution chemistry (pH and ionic strength), membrane properties (structural morphology and surface energy) and process conditions (temperature and hydrodynamic conditions) (Guo et al. 2012). In one of the current researches, the re-removal of biopolymers with molecular weight (MW) between 20 kDa and 100 kDa led to a lower rate of transmembrane pressure development by the UF membrane (Xu et al. 2021). Similarly, it was found that coagulation can improve the GDU membrane system performance by removing the dissolved organic compounds (Huang et al. 2021). In that case, for GDU with low pressure gradient, study on biopolymer fouling is crucial. However, in gravity-driven ultrafiltration membrane system, membrane flux is fouling and hydrostatic pressure dependence.

Ultra-low pressure gravity driven ultrafiltration (GDU) membrane system is potentially economical and less complex than conventional membranes for water applications (García-Pacheco et al. 2021). However, in the case of small scale or personal-used GDU membrane system, flux declination is a complex phenomenon because it is not only due to the fouling phenomena but also caused by the reducing hydrostatic pressure and availability of membrane surface area. In this work, GDU membrane system was tested on its separation efficiency by removing two major contaminants in the surface water namely humic acid and calcium carbonate solution which represent colour and turbidity, respectively. The aim of this study is to evaluate the GDU performance and fouling characteristic using UF hollow fibre PVDF membrane in treating the surface water. The performance in terms of flux and solute rejection were measured at regular intervals and correlate to the hydrostatic pressure depletion and reducing effective membrane area. A model was developed in order to predict the ideal dynamic flux performance and theoretically predict the fouling characteristic as well as concentration of the retentate over the time.

Materials And Methods

Preparation of Humic acid solution

Humic acid (HA) solution was prepared by dissolving predetermined amounts of the powdered HA, technical grade (SIGMA-ALDRICH, Switzerland) in deionized water produced by NANO Pure water purification system (Barnstead, Dubuque, IA) with resistivity greater than 18 MΩ -cm. The predetermined feed concentrations of the HA solutions are 10, 20, 30, 40 and 50 mg/L. The content of HA concentration was measured using a UV-Vis spectrophotometer (Cary 60, Agilent Technologies) with the absorbance at 254 nm. Solution pH was adjusted to pH 10 using 1 M NaOH stirred at a rate of 180-200 rpm for overnight. pH was measured using a pH/Conductivity Meter (EC500, ExTech Instruments).

Preparation of Calcium Carbonate solution

The synthetic calcium carbonate, $CaCO_3$ solutions were prepared by mixing the $CaCO_3$ powder in filtered deionized (DI) water produced by NANO Pure water purification system (Barnstead, Dubuque, IA) with resistivity greater than 18 MΩ -cm. Solution pH was reduced to pH 10 using 1 M HCl and the solution being stirred at a rate of 180-200 rpm for overnight. The pH was measured using a pH meter (EC500, ExTech Instruments). The predetermined feed concentrations of the $CaCO_3$ solutions are 0.1, 0.2, 0.3, 0.4 and 0.5 wt%. The concentration of $CaCO_3$ solution was calibrated against turbidity using Turbidity Meter (HANNA Instruments, Romania).

Real Water sampling

Real water sample was collected from Kerian River located at (5°09'50.2"N 100°28'35.0"E), Nibong Tebal, Penang. 8 liters of river water sample was collected to determine the total suspended solid (TSS), mixed liquor suspended solid (MLSS) and mixed liquor volatile suspended solid (MLVSS), Chemical Oxygen Demand (COD), pH, conductivity, turbidity, and hardness. Then, the river water sample was left for 24 hours settling and the supernatant was collected for the ultrafiltration process using the GDU membrane system.

Experimental setup and operating condition

The setup of bench top, dead-end gravitational driven ultrafiltration (GDU) membrane is shown in Fig. 1. The GDU membrane system comprises of 30 pieces of commercial Polyvinylidene Fluoride (PVDF) hollow fibre membranes (Hangzhou Waterland Environmental Technologies Co. Ltd., Zhejiang, China) with a length of 60 cm assembled vertically in a 30-cm-height tubular column in two-pass (folded membrane) to give total filtration area of 0.078585 m^2. Gravitational Driven Ultrafiltration (GDU) membrane system with inner diameter membrane fibre, outer diameter membrane fibre and nominal pore size distribution of 0.7 mm, 1.3 mm and 0.03 µm respectively. The column for the tubular hollow membrane module was made of polyvinyl chloride (PVC) pipe of 30.0 cm length and 0.3 cm thickness associated with internal diameter of 2.0 cm. The setup was placed on the bench with the retort stand to maintain the hollow fibre membrane module in the upright position to prevent any differences in hydrostatic pressure.

Different type of feeds was added to the membrane module from the top. The filtration was carried out in the batch mode with the feed solution filled up the module with total volume of 80 ml and let the solution level depleted throughout the ultrafiltration process. The membrane was operated based on outside-in mode. The permeate passed through the membrane wall into the lumen and collected at the bottom of the module. The ultrafiltration process was carried out using fresh and clean hollow fibre membrane for every type and concentration of feed solution without recycling or cleaning process. The modules were employed to filter two different feeds namely humic acid and calcium carbonate solution. The permeate was collected at the bottom of the column using 250 mL glass beaker and measured as weight using an electric balance (FX-3000i, A&D Company, Japan) connected to data-acquisition system. The retentate

was collected in a sample bottle at the end of the filtration process when the weight of permeate obtained become stationery where the membrane module was turned upside down then the retentate will flow out from the membrane module since it is a dead-end membrane system.

Analytical measurement

The turbidity of the calcium carbonate solution (before and after) the filtration was monitored using a Turbidity Meter (HANNA Instruments, Romania). The absorbance of humic acid was obtained using UV-Vis Spectrophotometer (Cary 60 UV Vis, Agilent Technologies) for the absorbing wavelength of humic acid is 254 nm. The concentration of humic acid solution was determined based on a calibration curve plotted for UV absorbance against the predeterminded concentrations. The particle size distribution was measured using a Malvern Zetasizer Nano ZS (Malvern Instrument Ltd., U. K.) by the DLS technique.

Membrane Characterization

The mean pore size distribution of the hollow fibre PVDF membrane was determined using Porometer (Porolux 1000). The morphology and composition of the deposit layer on both surface and cross-section, before and after the ultrafiltration process, were examined under scanning electron microscopy (FEI Quanta 450, United Stated), coupled with energy dispersion spectrometry (EDS, EDAX company, USA). The surface hydrophilicity of the fresh and fouled hollow fibre membranes were analysed using a dynamic contact angle analyser instrument via sessile droplet method. The contact angle using deionized water as probe liquid was anlyzed using Surface Meter (TM) version 1.2.1.9 (LAUDA Scientific) software. The contact angle was measured immediately after dropping 5 µl of deionised water. The contact angle of clean and fouled hollow fibre membrane by humic substances and calcites particulate were analysed. Three measurements were repeated to minimize its error and the results were reported as an average value (Hebbar et al. 2017; Kumar et al. 2013; Liu, et al. 2012).

Separation Efficiency Study

Two different type of feeds namely humic acid and calcium carbonate solution were fed from the top of the membrane module. The feed was filled up from the top of the membrane module. Before the filtration process started, all the membrane samples were rinsed using ethanol to reduce the water surface tension as well as the additives of the hollow fibre PVDF membrane. After that, the membrane was fed with deionized water to remove the remaining ethanol. The initial water flux, J (L/(m^2/h)) was calculated according to Eq. 1:

$$\text{Flux, J (L/m}^2\text{h)} = \frac{V}{A\Delta t} \quad (1)$$

Where V, A and Δt represent the volume of permeated water, the membrane area and the permeation time, respectively. The membrane flux was calculated by dividing the collected weight over the predetermined time and the filtration area. The retention capability was measured for humic acid solution and calcium

carbonate solution. Thus, the observed solute rejection percentage (R) was calculated from the following equation:

$$\text{Rejection, R}(100\%) = (1 - \frac{C_p}{C_f}) \text{ x } 100\% \quad (2)$$

Whereby R is rejection, C_p and C_f are the concentration of contaminants in the permeate and feed, respectively. All the results presented are average data from three samples of each concentration of feed.

Dynamic Membrane Filtration Modelling

The performance of the GDU system under dead-end mode was varied over the time under depleting hydrostatic pressure, membrane area as well as membrane fouling. By assuming linear pressure drop across the membrane wall thickness, the flow characteristic of the fluid across the porous membrane can be described by Darcy law (Eq. 3). The flow rate is controlled by the permeability (k') and directly proportional to the hydrostatic pressure (P) across the membrane thickness (Δx) and varied along the length of the membrane consisting of membrane contacting the solution:

$$J = k' \frac{dP}{dx}$$

3

The pressure (hydrostatic pressure) experienced by the hollow fibre in the feed is varied according to the level of the solution, z. It was assumed that the flow rate is directly proportional to the hydrostatic pressure along the length of the filtration module containing hollow fibre PVDF membrane. At any point on the membrane surface, h, the total flux of n fibres with radius r can be expressed as:

$$JdA_m = \frac{-k'(z-h)\rho g}{\Delta x} d(n2\pi rh)$$

4

$$\int JdA_m = \int \frac{-k'\rho g 2\pi r}{\Delta x}(z-h)\,dh = \int_{h=z}^{h=0} -k''(z-h)\,dh = \frac{k''z^2}{2};\ k'' = \frac{k'\rho g 2\pi rn}{\Delta x} \quad (5)$$

The flux profile in this case is the characteristic of the membrane which can be modelled based on Reynold Transport Theorem.

\frac{\partial }{\partial t}\int dV=-\int vd{A}_{m}

6

Where V is the the control volume, A_m is the area of the control surface and v is the velocity of the fluid crossing the control surface.

The water permeability coefficient, k' can be determined from Eq. (4) and E. (5) through the permeability of filtration membrane with the thickness of the membrane divided by the density, gravitational force of the total surface area of overall membrane filtration using the following equation.

$k' = \frac{k\text{'}\text{'}\varDelta x}{pg2\pi rn}$ (7)

where k'' represented the permeability of the filtration membrane, \varDelta x is the thickness of the membrane, p is the density and g is the gravitational force.

The height of the feed solution inside the membrane module throughout the ultrafiltration process, at any time, can be estimated by using equation below:

$$\left({A}_{T}-{nA}_{F}\right)\frac{dz}{dt}=-\frac{k"{z}^{2}}{2}$$
8
$${\int }_{{z}_{o}}^{z}\frac{1}{{z}^{2}}dz={\int }_{0}^{t}\frac{-k"}{2\left({A}_{T}-{nA}_{F}\right)}dt$$
9
$${\left.-\frac{1}{z}\right|}_{{z}_{o}}^{z}=\frac{-k"t}{2\left({A}_{T}-n{A}_{F}\right)}$$
10
$$\frac{1}{z}-\frac{1}{{z}_{o}}=\frac{k"t}{2\left({A}_{T}-n{A}_{F}\right)}$$
11
Where A_T is the cross-sectional area of the module, A_F is the cross-sectional area of the fibre, z is the water level at time t and z_o is the initial water level.

In order to investigate the membrane and foulant characteristic, total resistance of membrane and cake layer can be determined from the fitted k' value. The permeability of the membrane filtration, k' can be calculated as shown in the following equation (for pure water).

$$\frac{{k}^{\text{'}}}{\varDelta x}=\frac{1}{\mu \left(Rm\right)}$$
12
where μ is the dynamic viscosity and R_m is the membrane resistance. The total resistance due to membrane and cake resistance (R_m + R_c) can be determined by measuring the permeability of feed solution:

$$\frac{{k}^{\text{'}}}{\varDelta x}=\frac{1}{\mu (Rm+Rc)}$$
13
Assuming no adsorption on the membrane surface with perfect rejection, the ideal concentration of the feed solution, can be predicted as below:

$$cz={c}_{o}{z}_{o}$$
14
$$\frac{c}{{c}_{o}{z}_{o}}-\frac{1}{{z}_{o}}=\frac{k"t}{2\left({A}_{T}-{nA}_{F}\right)}$$
15
$$c={c}_{0}\left[1+\frac{k"t{z}_{o}}{2\left({A}_{T}-n{A}_{F}\right)}\right]$$
16
Where A_T = cross sectional area of module/pipe, A_F=cross sectional area of single fibre; A_m= surface area of membrane, n=number of fibers; r = radius of fiber; z= water level, h = height of membrane

Real Water quality analysis

Water quality analysis parameters such as Chloride, Ammonia, Nitrate, Nitrite, sulphate, hardness and Chemical Oxygen Demand (COD) were measured using Photometer System (MaxiDirect, Lovibond, Germany) with the aids from the detection reagent, tablet and powder provided for each parameter. Meanwhile, pH, conductivity and TDS were determined and calibrated using pH and Conductivity Meter (HANNA Instruments, Romania).

Results And Discussions

GDU membrane performance of humic acid as feed solution

To determine the performance of the GDU process, permeation flux of HA with different concentrations were evaluated. Membrane fouling was aggravated with the increased of HA concentration which led to lower flux and poorer membrane rejection. Fig. 2 shows that the average membrane rejection (triplicate results) declined from 94.96–90.39% as the initial concentration of HA (mg/L) increased from 10 mg/L to 50 mg/L, indicating that HA penetration was taken placed and its permeation was driven by the concentration gradient. It was found that membrane fouling via surface adsorption had caused the considerable HA permeation as indicated by the reduction of rejection capability.

Based on Fig. 3, the highest flux produced by HA solution was 2.07 kg/m^2s with initial humic acid concentration of 10 mg/l. The system took about 400 s to totally wet the membrane pores. As mentioned earlier, flux reduction was due to the combined effects of fouling and depleting hydrostatic pressure. Flux reduction could be contributed by both reversible (concentration polarization) and irreversible (adsorption and deposition) fouling. Concentration polarization resulted in flux drop due to the reduction in the effective pressure (driving force). Concentration polarization become more crucial for dissolved solute separation as osmotic pressure is concentration dependence (Taheri et al. 2013). However, in this case, concentration polarization is not the controlling parameter for UF process. Instead, cake layer deposition is the dominating flux reduction factor. The membrane-filled module required 60 minutes to empty the whole solution and it is almost independent of the concentration of HA being used. This showed that concentration polarization was not the main cause of flux declination. However, it was also found out that the onset of fouling is proportional to the initial feed concentrations of HA. The higher the HA concentrations, the faster the onset of the fouling. Another interesting phenomenon observed from the graph was the initial declination slopes were almost similar which showed that the physical characteristic of the HA cake layer is quite similar under such a low-pressure operation.

The retentate solution concentrations are shown in Table 1. For the initial 10 mg/L of HA, the final retentate being concentrated to 69.74 mg/L which was about 7 times increased in feed concentration. Same goes to the initial feed concentrations of 20, 30 and 40 mg/L of humic acid. The concentration of retentate solution (50 mg/L) solution increased approximately 8 times to 378.90 mg/L compared to the

initial feed concentration at the end of experiment. The HA was rejected via retention as well as surface adsorption. In that case, at higher HA feed concentration, the tendency for the solution to retain rather than adsorb on the membrane surface is more prevalent. It is because at higher initial feed concentration, the solubility of the HA was getting lower and it tends to appear as bigger aggregated molecule in the bulk solution (Rucka et al. 2019). In overall, the results showed that the HF membrane could retain the HA well even under gravitational driving force.

Table 1
Concentrated HA retained in the membrane module

Initial Feed Concentration (mg/L)	Retentate solution concentration (mg/L)	Concentrating Factor
10.0	69.74 ± 0.12	6.97
20.0	134.17 ± 0.46	6.71
30.0	197.97 ± 0.46	6.60
40.0	259.33 ± 0.39	6.67
50.0	378.90 ± 0.30	7.58

The size distribution of HA was measured using Zetasizer nano series instrument under room temperature. The mean apparent size distribution of aggregated HA was 2.443 μm. The aggregated HA cannot pass through the membrane pores with smaller pore size (0.03 micron) due to size exclusion. However, the dissolved humic substances have molecular weight around 1 kDa which could easily permeate through the membrane. Thus, dissolved HA could not be rejected effectively by the membrane (Jeong et al. 2014).

GDU membrane performance of Calcium Carbonate as feed solution

Figure 4 shows that the rejection of $CaCO_3$ was higher than 97% with the initial feed concentration lower than 0.5 wt%. The rejection capability of the membrane reduced from 99.19 to 97.41% when the concentration of $CaCO_3$ was increased from 0.1 to 0.5 wt %. Overall, its rejection capability towards calcium carbonate was higher than humic acid. The same separation principle applied whereby the higher the concentration gradient, the higher the mass transfer of the solute across the membrane. The higher the $CaCO_3$ concentration, the tendency for it to scale the membrane become higher (Wang et al. 2013). The percentage of removal showed that the rejection of $CaCO_3$ is significantly reduced if its concentration was increased.

Figure 5 shows that the onset of scaling by $CaCO_3$ solution was also concentration dependent. The higher the $CaCO_3$ concentration, the onset of scaling would be faster and subsequently the flux declined faster after the onset point. This mean that the physical characteristic of the cake layer is also concentration dependent. The higher the concentration of the $CaCO_3$, the denser of the cake layer. The formation of cake layer reduced the membrane flux over the time. Figure 5 shows that the highest flux of

2.81 L/m^2.hr was obtained when 0.1 wt% $CaCO_3$ solution was filtered. Meanwhile, the lowest flux was recorded as 2.31 L/m^2hr when 0.5 wt % $CaCO_3$ was filtered. Nonetheless, the fouling of $CaCO_3$ is not as serious as humic substance due to its different cake layer characteristic. $CaCO_3$ crystallization could be initiated on the membrane surface or in the bulk solution followed by surface deposition. However, its deposition characteristic could be different for such a low-pressure environment. Based on the zeta sizer result, the mean size distribution of $CaCO_3$ was 4.793 µm which is much larger compare to HA aggregate. In view of this, it was deduced that $CaCO_3$ precipitation had led to a thicker but looser cake layer compared to humic acid. The concentrated calcium carbonate retained in the membrane module is shown in Table 2. The $CaCO_3$ at 0.5 wt% showed a drastic increased of concentrating factor which indicated that the early onset of fouling prevents the removal of $CaCO_3$.

Table 2
Concentrated $CaCO_3$ retained in the membrane module

Initial Feed Concentration (wt%)	Retentate solution concentration (wt%)	Concentrating Factor
0.1	4.77 ± 0.08	47.67
0.2	10.85 ± 0.10	54.23
0.3	11.65 ± 0.10	38.83
0.4	17.78 ± 0.20	44.44
0.5	61.96 ± 0.40	123.92

Surface fouling analysis

Scanning electron microscope (SEM) is a common technique used for characterizing the morphology of membranes before and after fouling. Fig. 6 shows that after the humic substance filtration, some sparingly soluble salts were found deposited on the surface of the hollow fibre membrane. It was loosely packed and dispersive, and the colour of the membrane surface became brown (observed using naked eye). The SEM-EDX analysis of the surface showed that 7.73 wt% of Oxygen (O), 0.91 wt% of Silicates (Si), 1.01 wt% Magnesium (Mg) and 0.43 wt% Aluminium (Al) were the deposit materials associated with the humic acid structure and its associated components. Humic substance was more favourably adsorbed onto hydrophobic membranes due to the hydrophobic interaction. Similar to the $CaCO_3$ precipitation, HA deposition can be initiated on the surface by the free humic substance or precipitated from the bulk solution (Mitrouli et al. 2016).

Figure 7 shows the SEM image of $CaCO_3$ precipitation on the hollow fibre PVDF membrane surface after filtration. The precipitated $CaCO_3$ led to the loose scaling layer due to the absence of high pressure. From the SEM-EDX analysis, the deposit on the membrane surface was mainly Calcium (Ca) and Silicates (Si) consists of 5.55 wt% and 2.27 wt% respectively. These irregular structures are the amorphous $CaCO_3$

particles, while growing, tend to be transformed into the stable regular crystals over the time (Mitrouli et al. 2016; Mitrouli et al. 2016).

The rejection performance of the membranes was accordance to the particle size of the foulants. The membrane gave the highest rejection towards $CaCO_3$ and followed by humic substance according to the size of the precipitate. Furthermore, it is important to note that the higher permeation velocity could lead to solute concentrating at membrane surface that favours nucleation and crystal growth (Mitrouli et al. 2016). Under such a low-pressure filtration, cake layer formation is favoured over the pore blocking which indicated that the fouling could be reversible (Xu et al. 2012).

Water Contact Angle Analysis

Surface hydrophilicity is one of the most important properties of membrane which could affect the flux and antifouling ability of the membrane (Kim et al. 2003; Lu et al. 2008; Oh et al. 2009). Contact angle value also indicates the membrane material affinity to water. As shown in Table 3, the contact angle value of the membrane surface increased significantly with different type of foulants. The increased contact angle value was due to the increased of surface roughness after surface precipitation. The contact angle of pristine PVDF membrane was 67.20˚ ± 1.09, after HA precipitation, the contact angle increased to 81.88˚ ± 0.74. Similarly, after ultrafiltration of $CaCO_3$, the contact angle was increased to 87.47˚ ± 0.72. The heterogeneous nucleation and growth processes on the of calcite materials was the dominating structure during the incipient scaling process (Vela et al. 2008). increased of contact angle upon fouling is not favorable as it requires to overcome the extra capillary force of water permeating the pores.

Table 3
Contact angle value of DGU membrane towards different feeds solution

Hollow Fibre (HF) Membrane	Contact Angle (˚)
Pristine HF PVDF membrane	67.20 ± 1.09
HF membrane after filtration of Humic Acid	81.88 ± 0.74
HF membrane after filtration of Calcium Carbonate	87.47 ± 0.72

Cake layer resistance analysis

Table 4 displays the variation of total resistance under varying concentration of the feed solutions under gravitational driven membrane filtration. After running the filtration using two different feed solution, membrane resistance, R_m was estimated as 2.17×10^{10} m^2/kg which is close to the value reported by Piry et al., with the membrane resistance, R_m ranging from 7.0×10^{10} to 8.9×10^{10}. However, in their study, the flux resistance was barely affected by the deposit layer formation. It was found that the cake resistance

(R_c) decreased under higher transmembrane pressure which means that some of the substances causing pressure-independent fouling are washed away (Piry et al. 2012).

Membrane fouling is started from the foulant deposition followed by cake layer build-up (Shao et al. 2017), the cake fouling resistance, R_c accounted for 76.4 to 99.1% of the total fouling resistance. The higher ratio of cake fouling resistance suggested that the characteristic of cake layer was playing the role in determining the flux of the GDU system. This finding is detrimental to the GDU system with poor hydrodynamic condition. According to Di Profio et al., they observed that cake layer forms on the membrane surface result in R_c value of (x 10^{12}) for seawater filtration (Di Profio et al. 2011). and Listiarini et al. reported that the R_c value (x 10^{13}) for humic acid, bromide and bromate filtration (Listiarini et al. 2010). In this work, the cake layer resistance had the value of at least one order of magnitude lower than their reported value which indicated that the cake layer resistance was much lower for a GDU process compared to the pressure driven process.

Table 4 HF membrane resistance value of GDU membrane system towards (a) HA and (b) $CaCO_3$ filtration

(a)

Concentration	k" (m^3/s)	k' (kg/m^2s)	R_m (m^2/kg)	R_c (m^2/kg)
10 mg/L	$3.05x10^{-6}$	$3.65x10^{-13}$	$2.17x10^{10}$	$4.53x10^{11}$
20 mg/L	$2.11x10^{-6}$	$2.53x10^{-13}$	$2.17x10^{10}$	$6.62x10^{11}$
30 mg/L	$2.08x10^{-6}$	$2.50x10^{-13}$	$2.17x10^{10}$	$6.71x10^{11}$
40 mg/L	$2.06x10^{-6}$	$2.47x10^{-13}$	$2.17x10^{10}$	$6.79x10^{11}$
50 mg/L	$1.65x10^{-6}$	$1.98x10^{-13}$	$2.17x10^{10}$	$8.52x10^{11}$

(b)

Concentration	k" (m^3/s)	k' (kg/m^2s)	R_m (m^2/kg)	R_c (m^2/kg)
0.1 wt%	$2.03x10^{-5}$	$2.44x10^{-12}$	$2.17x10^{10}$	$4.92x10^{10}$
0.2 wt%	$1.68x10^{-5}$	$2.02x10^{-12}$	$2.17x10^{10}$	$6.40x10^{10}$
0.3 wt%	$1.60x10^{-5}$	$1.91x10^{-12}$	$2.17x10^{10}$	$6.89x10^{10}$
0.4 wt%	$1.46x10^{-5}$	$1.75x10^{-12}$	$2.17x10^{10}$	$7.72x10^{10}$
0.5 wt%	$1.27x10^{-5}$	$1.53x10^{-12}$	$2.17x10^{10}$	$9.15x10^{10}$

Table 4 shows the variation of the filter cake resistance, R_c for humic acid and calcium carbonate solution. In this study, the resistance of cake layer, R_c was found to be increased as the concentration of feed solution increased. Amongst the feed solutions, humic acid solution gave the highest filter cake resistance, R_c of 8.52x10^{11} m^2/kg. This is in accordance to the previous SEM image that the cake layer is denser due to its smaller mean size distribution of HA (2.443 μm) compared to the calcium carbonate (4.793 μm). On the other hand, $CaCO_3$ had the lowest R_c of 4.92x10^{10} m^2/kg. This finding is in accordance to our previous flux declination result. As compared to humic substance, precipitated $CaCO_3$ produced more porous layers due to its irregular particulate size.

Permeability analysis

Figure 8 shows the changes of permeability for the feed solution under different feed concentrations. It can be observed that the *k'* value (m^3/s) of the foulants were having an order of magnitude differences for different type of feed. The lowest *k'* value (x 10^{-6}) was recorded for the HA filtration and the $CaCO_3$ filtration which appeared in particulate materials has the highest permeability (x 10^{-5}). The inorganic substance, $CaCO_3$ formed irregular particulate materials that enabling the maximum water permeation through the loose cake layer on the membrane surface. Thus, this layer in fact gave a much denser cake layer for the water permeation.

All the foulants showed that the water permeability decreased with the increased of feed concentrations (She et al. 2016; Shi et al. 2020). The turbidity showed that the permeability decreased almost linearly with the concentration. On the other hand, humic substance showed a non-linear decreasing trend of the permeability against feed concentration. The rapid decrease of permeability against the concentration of HA indicated that the fouling of HA might be contributed by both the cake layer as well as membrane adsorption by the free HA via hydrophobic interaction. The reduction of HA permeability in higher feed concentration can be attributed to aggregation and cake formation (Costa and de Pinho 2005; Sutzkover-Gutman et al. 2010).

Concentrating Effect of dead End GDU membrane system

Figure 9 is the simulated ideal concentration of solution (being concentrated) in the filtration module over the time. Based on Fig. 9, the concentration profile is linear and permeability (*k"*) dependant. The higher the *k"* value, the faster the solution being concentrated. The concentration of two feed solution including humic acid and calcium carbonate solution were estimated using Eq. 16 and compared to the actual concentration in the filtration module after the filtration time of 1 hour 40 minutes.

According the results shown in Table 1, for HA, the predicted concentration remains in membrane module by the developed model was in the range of 69.74 to 378.90 mg/L compared to the calculated concentration of HA in membrane module was about 10.89 to 521.53 mg/L. The calculated

concentration $CaCO_3$ was 4.77 to 61.96 wt % while the predicted $CaCO_3$ concentration was around 1.13 to 78.76 wt %. From the obtained results, it was found that the ideal calculated concentrations for low concentrations feed was always lower than the experimentally determined concentration. On the other hand, at higher concentration, the calculated concentration was higher than the measured value. This indicated that for low concentration, the permeability constant is not dominated by the cake layer, so the actual permeability is higher than the predicted value. In contrary, at higher feed concentration, due to the rapid fouling, the concentration of the retentate is lower than the ideal conditions due to the adsorption of solutes on the membrane surface during fouling.

Real water filtration using the GDU membrane system

The purpose of carrying out the river water test was to assess the removal efficiencies of the impurities presence in the river water. For that purpose, 80 mL of the river water sample was filtered with no water circulation. The solution in the module was emptied naturally as the feed was done once. Based on Fig. 10, the maximum flux of 45.98 L/m^2hr could be achieved around 500 s after which sharp flux drop was seen. The flux dropped approximately 52.47% from 45.98 to 21.86 L/m^2hr within 500 s after the maximum flux. Then, the slope become gradually decreased to the lowest flux of 0.86 L/m^2hr indicating the depleting hydrostatic pressure. Generally accepted membrane filtration theory assumes that the formation of fouling layer during ultrafiltration led to a continuous increase of hydraulic resistance and decreases of flux (Wang et al. 2019).

Table 5 shows the water quality analysis obtained from the ultrafiltration process. The results indicated that the GDU membrane system is able to polish the river water and produce permeate with better quality. The ultrafiltration process using GDU membrane system efficiently removed the contaminants or foulant of the feed river water including chloride, ammonia, nitrate, nitrite, sulphate, chemical oxygen demand (COD) and also turbidity, pH, conductivity and total dissolved solid (TDS).

During the experiment, partial reduction of chloride, ammonia, nitrate, nitrite and sulphate concentration were observed. Chloride was reduced from 4.73 ± 0.35 mg/L to 2.43 ± 0.25 mg/L which result in 48.63% removal while ammonia content dropped to 0.08 mg/L ± 0.01 from the initial concentration of 0.13± 0.02 mg/L. Ultrafiltration is known to be the membrane that has poor retention on the dissolved ionic salt due to its bigger pore size. Although at the beginning, the chemical oxygen demand (COD) was 22.33 ± 1.53 mg/L, settlement assisted GDU membrane system was able to reduce the COD to an undetectable level showing that the organic matter content can be effectively removed. COD is a crucial parameter in determining the water quality that represent organic loading in the water (Verma and Singh 2013).

Table 5
Water Quality Analysis for Kerian River Filtration Process

Parameter	Before Filtration	After Filtration
Chloride (mg/L)	4.73 ± 0.35	2.43 ± 0.25
Ammonia (mg/L)	0.13 ± 0.02	0.08 ± 0.01
Nitrate (mg/L)	Below 4 mg/L	Below 4 mg/L
Nitrite (mg/L)	0.04 ± 0.01	Below 0.01 mg/L
Sulphate (mg/L)	Below 5 mg/L	Below 5 mg/L
Hardness (mg/L)	16.33 ± 1.53	10.0 ± 1.0
COD (mg/L)	22.33 ± 1.53	Below 0 mg/L
Turbidity (NTU)	46.53 ± 0.15	0.25 ± 0.02
pH	7.45 ± 0.02	7.20 ± 0.03
Conductivity (µS/cm)	63.90 ± 0.02	58.97 ± 0.59
TDS (mg/L)	31.93 ± 0.306	29.50 ± 0.265

Unexpectedly, merely 60% of the hardness in the river can be removed which indicated that the hardness may be in a more dissolved form. On the other hand, the feed turbidity dropped significantly from an initial value of 46.53 to 0.25 NTU which showed that GDU membrane is very effective in suspended solid removal. For the other parameter such pH, conductivity and TDS, no significant changes and slightly fluctuation in the permeate quality were observed due to their smaller size. It can be concluded that the proposed system is effective in removing solid and bigger organic molecule which is a typical performance of ultrafiltration membrane (Wang et al. 2019).

Conclusion

In this study, the filtration performance of modular GDU membrane system under depleting hydrostatic pressure and reducing available active layer were evaluated and the fouling development on the hollow fibre PVDF UF membrane was monitored. This study discloses that the PVDF ultrafiltration membrane could highly reject calcium carbonate than humic acid. Membrane fouling is inevitable especially with higher feed concentrations. It was also observed that the membrane resistance is lower than the cake layer resistance. In this case, under the low hydrostatic pressure, they were prone to be surface cake layer fouling but at much lower magnitude compared to the pressure difference process. The dynamic modelling showed that amongst the foulants, the humic substances could reduce the membrane permeability at larger extent due to the HA aggregate which cannot pass through the membrane with smaller pore size and formed denser cake layer whereas the permeability of the $CaCO_3$ was higher due to its irregular particulate materials that loosen the cake layer. The flux profile of actual river water filtration

showed that the proposed GDU membrane system could be effective in removing the turbidity and COD from the river water.

Declarations

Funding

This work was supported by the Malaysia Research University Network (MRUN) Collaborative Research Program (203/PJKIMIA/67216003), Ministry of Higher Education Malaysia.

Declaration of interests

The authors declare that they have no known competing financial interests or personal relationships that could have appeared to influence the work reported in this paper.

Authors Contributions

Nur IR Imani Ishak : Data curation, Writing- Original draft preparation.

Ooi Boon Seng : Conceptualization, Reviewing, Editing, Supervision

Derek Chan Jiunn Chieh : Reviewing and Editing

Acknowledgements

This work was supported by the Malaysia Research University Network (MRUN) Collaborative Research Program (203/PJKIMIA/67216003), Ministry of Higher Education Malaysia.

Ethical Approval

Not Applicable

Consent to Participate

Not Applicable

Consent to Publish

Not Applicable

Availability of data and materials

The datasets generated during and/or analysed during the current study are available from the corresponding author on reasonable request.

References

1. Akhondi E, Wu B, Sun S, Marxer B, Lim W, Gu J, Liu L, Burkhardt MMcDougald D, Pronk Fane W AG (2015) Gravity-driven membrane filtration as pretreatment for seawater reverse osmosis: Linking biofouling layer morphology with flux stabilization. Water Res 70:158–173
2. Chomiak A, Traber J, Morgenroth E, Derlon N (2015) Biofilm increases permeate quality by organic carbon degradation in low pressure ultrafiltration. Water Res. 85: 512-520
3. Costa AR, de Pinho MN (2005) Effect of membrane pore size and solution chemistry on the ultrafiltration of humic substances solutions.J. of Membr. Sci.255:49–56
4. Derlon N, Grütter A, Brandenberger F, Sutter A, Kuhlicke U, Neu TR, Morgenroth E (2016) The composition and compression of biofilms developed on ultrafiltration membranes determine hydraulic biofilm resistance.Water Res.102:63–72
5. Derlon N, Koch N, Eugster B, Posch T, Pernthaler J, Pronk W, Morgenroth E (2013) Activity of metazoa governs biofilm structure formation and enhances permeate flux during Gravity-Driven Membrane (GDM) filtration.Water Res.47:2085–2095
6. Derlon N, Peter-Varbanets M, Scheidegger A, Pronk W, Morgenroth E (2012) Predation influences the structure of biofilm developed on ultrafiltration membranes.Water Res.46:3323–3333
7. Di Profio G, Ji X, Curcio E, Drioli E (2011) Submerged hollow fiber ultrafiltration as seawater pretreatment in the logic of integrated membrane desalination systems.Desalination.269:128–135
8. Ding A, Wang J, Lin D, Tang X, Cheng X, Wang H, Bai L, Li G, Liang H (2017) A low pressure gravity-driven membrane filtration (GDM) system for rainwater recycling: Flux stabilization and removal performance.Chemosphere.172:21–28
9. García-Pacheco R, Li Q, Comas J, Taylor RA, Le-Clech P (2021) Novel housing designs for nanofiltration and ultrafiltration gravity-driven recycled membrane-based systems.Sci. of The Total. Env.767:144181
10. Guo W, Ngo H-H, Li J (2012) A mini-review on membrane fouling.Bioresour. Technol.122 -34
11. Hebbar RS, Isloor AM, Ismail AF *Chapter 12 - Contact Angle Measurements*, in, ed, in Membrane Characterization E (2017)182–203
12. Huang Y, Cheng P, Tan FJ, Huang Y, Li P, Xia S (2021) Effect of coagulation pretreatment on the performance of gravity-driven membrane filtration with Yangtze River water.Journal of Cleaner Production.297:126736
13. Jeong S, Rice SA, Vigneswaran S (2014) Long-term effect on membrane fouling in a new membrane bioreactor as a pretreatment to seawater desalination.Bioresour. Technol.165:60–68
14. Kim SH, Kwak S-Y, Sohn B-H, Park TH (2003) Design of TiO2 nanoparticle self-assembled aromatic polyamide thin-film-composite (TFC) membrane as an approach to solve biofouling problem.J. of Membr. Sci.211:157–165
15. Kohler E, Villiger J, Posch T, Derlon N, Shabarova T, Morgenroth J, Blom JF Biodegradation of microcystins during gravity-driven membrane (GDM) ultrafiltration.PLoS One.9:e111794

16. Kumar R, Isloor AM, Ismail AF, Rashid SA, Matsuura T (2013) Polysulfone–Chitosan blend ultrafiltration membranes: preparation, characterization, permeation and antifouling properties.RSC Adv.3:7855–7861
17. Listiarini K, Tor JT, Sun DD, Leckie JO (2010) Hybrid coagulation–nanofiltration membrane for removal of bromate and humic acid in water.J. of Membr. Sci.365:154–159
18. Liu J, Lu X-L, Wu C-R (2012) Effect of annealing conditions on crystallization behavior and mechanical properties of NIPS poly(vinylidene fluoride) hollow fiber membranes. J. of Appl. Polym. Sci. 129: 1417-1425
19. Lu C-H, Wu W-H, Kale RB (2008) Microemulsion-mediated hydrothermal synthesis of photocatalytic TiO2 powders.J. of Hazard. Mater.154:649–654
20. Mekonnen MM, Hoekstra AY (2016) Four billion people facing severe water scarcity.Science advances. 2: e1500323
21. Meng F, Chae S-R, Drews A, Kraume M, Shin H-S, Yang F (2009) Recent advances in membrane bioreactors (MBRs): Membrane fouling and membrane material.Water Res.43:1489–1512
22. Mitrouli ST, Kostoglou M, Karabelas AJ (2016) Calcium carbonate scaling of desalination membranes: Assessment of scaling parameters from dead-end filtration experiments.J. of Membr. Sci.510:293–305
23. Mitrouli ST, Kostoglou M, Karabelas AJ, Karanasiou A (2016) Incipient crystallization of calcium carbonate on desalination membranes: dead-end filtration with agitation.Desalination and Water Treat. 57:2855–2869
24. Oh SJ, Kim N, Lee YT (2009) Preparation and characterization of PVDF/TiO2 organic– inorganic composite membranes for fouling resistance improvement.J. of Membr. Sci.345:13–20
25. Peter-Varbanets M, Gujer W, Pronk W (2012) Intermittent operation of ultra-low pressure ultrafiltration for decentralized drinking water treatment.Water Res.46:3272–3282
26. Peter-Varbanets M, Hammes F, Vital M, Pronk W (2010) Stabilization of flux during dead- end ultra-low pressure ultrafiltration.Water Res.44:3607–3616
27. Peter-Varbanets M, Margot J, Traber J, Pronk W (2011) Mechanisms of membrane fouling during ultra-low pressure ultrafiltration.J. of Membr. Sci.377:42–53
28. Piry A, Heino A, Kühnl W, Grein T, Ripperger S, Kulozik U (2012)Effect of membrane length membrane resistance, and filtration conditions on the fractionation of milk proteins by microfiltration.J. of Dairy Sci.95:1590–1602
29. Pronk W, Ding A, Morgenroth E, Derlon N, Desmond P, Burkhardt M, Wu B, Fane AG (2019) Gravity-driven membrane filtration for water and wastewater treatment: A review.Water Res.149:553–565
30. Rucka K, Solipiwko-Pieścik A, Wolska M (2019) Effectiveness of humic substance removal during the coagulation process.SN Appl. Sci.1:535
31. Shao S, Feng Y, Yu H, Li J, Li G, Liang H (2017) Presence of an adsorbent cake layer improves the performance of gravity-driven membrane (GDM) filtration system.Water Res.108:240–249

32. She Q, Wang R, Fane AG, Tang CY (2016) Membrane fouling in osmotically driven membrane processes: A review.J. of Membr. Sci.499:201–233
33. Shi D, Liu Y, Fu W, Li J, Fang Z, Shao S (2020) A combination of membrane relaxation and shear stress significantly improve the flux of gravity-driven membrane system.Water Res.175:115694
34. Sutzkover-Gutman I, Hasson D, Semiat R (2010) Humic substances fouling in ultrafiltration processes. Desalination. 261: 218-231
35. Taheri AH, Sim LN, Haur CT, Akhondi E, Fane AG (2013) The fouling potential of colloidal silica and humic acid and their mixtures. J. of Membr. Sci. 433: 112-120
36. Tang X, Zhu X, Huang K, Wang J, Guo Y, Xie B, Li G, Liang H (2021) Can ultrafiltration singly treat the iron- and manganese-containing groundwater?J. of Hazard. Mater.409:124983
37. Tobias A, Bérubé PR (2020) Contribution of biofilm layer to virus removal in gravity-driven membrane systems with passive fouling control.Sep. and Purif. Technol.251:117336
38. Vela MCV, Blanco S, García JL, Rodríguez EB (2008) Analysis of membrane pore blocking models applied to the ultrafiltration of PEG.Sep. and Purif. Technol.62:489–498
39. Verma AK, Singh TN (2013) Prediction of water quality from simple field parameters Environmental Earth Sciences. 69:821–829
40. Wang H-C, Cui D, Han J-L, Cheng H-Y, Liu W-Z, Peng Y-Z, Chen Z-B (2019) Wang A-J A2O-MBR as an efficient and profitable unconventional water treatment and reuse technology: A practical study in a green building residential community. Resources, Conservation and Recycling. 150: 104418
41. Wang H, Alfredsson V, Tropsch J, Ettl R, Nylander T (2013) Formation of CaCO3 Deposits on Hard Surfaces—Effect of Bulk Solution Conditions and Surface Properties.ACS Appl. Mater. & Interfaces.5:4035–4045
42. Wang J, Ren H, Li X, Li J, Ding L, Geng J, Xu K, Huang H, Hu H (2018) In situ monitoring of wastewater biofilm formation process via ultrasonic time domain reflectometry (UTDR).Chem. Eng. J.334:2134–2141
43. Wang Y, Fortunato L, Jeong S, Leiknes T (2017)Gravity-driven membrane system for secondary wastewater effluent treatment: Filtration performance and fouling characterization.Sep. and Purif. Technol.184:26–33
44. Xu J, Ruan LG, Wang X, Jiang YY, Gao LX, Gao JC (2012) Ultrafiltration as pretreatment of seawater desalination: Critical flux, rejection and resistance analysis.Sep. and Purif. Technol.85:45–53
45. Xu L, Zhou Z, Graham NJD, Liu M, Yu W (2021) Enhancing ultrafiltration performance by gravity-driven up-flow slow biofilter pre-treatment to remove natural organic matters and biopolymer foulants.Water Res.195:117010
46. Zhang J, Zhang L, Miao Y, Sun Y, Li X, Zhang Q, Peng Y (2018) Feasibility of in situ enriching anammox bacteria in a sequencing batch biofilm reactor (SBBR) for enhancing nitrogen removal of real domestic wastewater. Chem. Eng. J. 352: 847-854

Figures

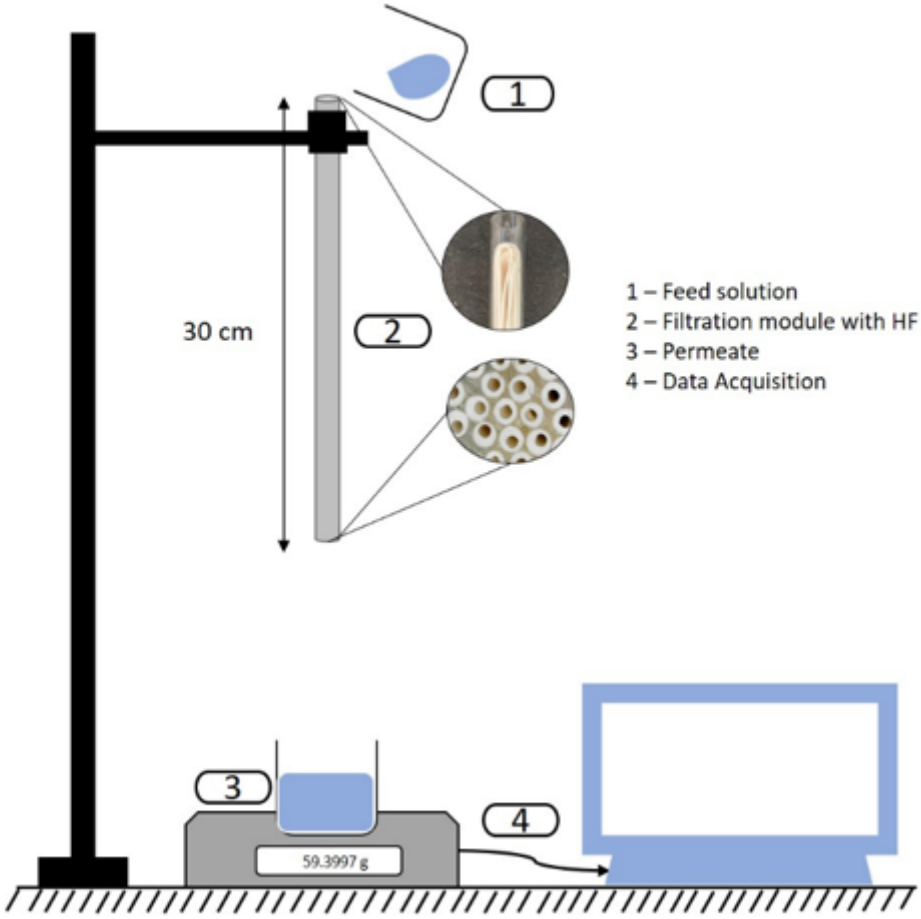

Figure 1

The bench top gravitational driven ultrafiltration (GDU) membrane system

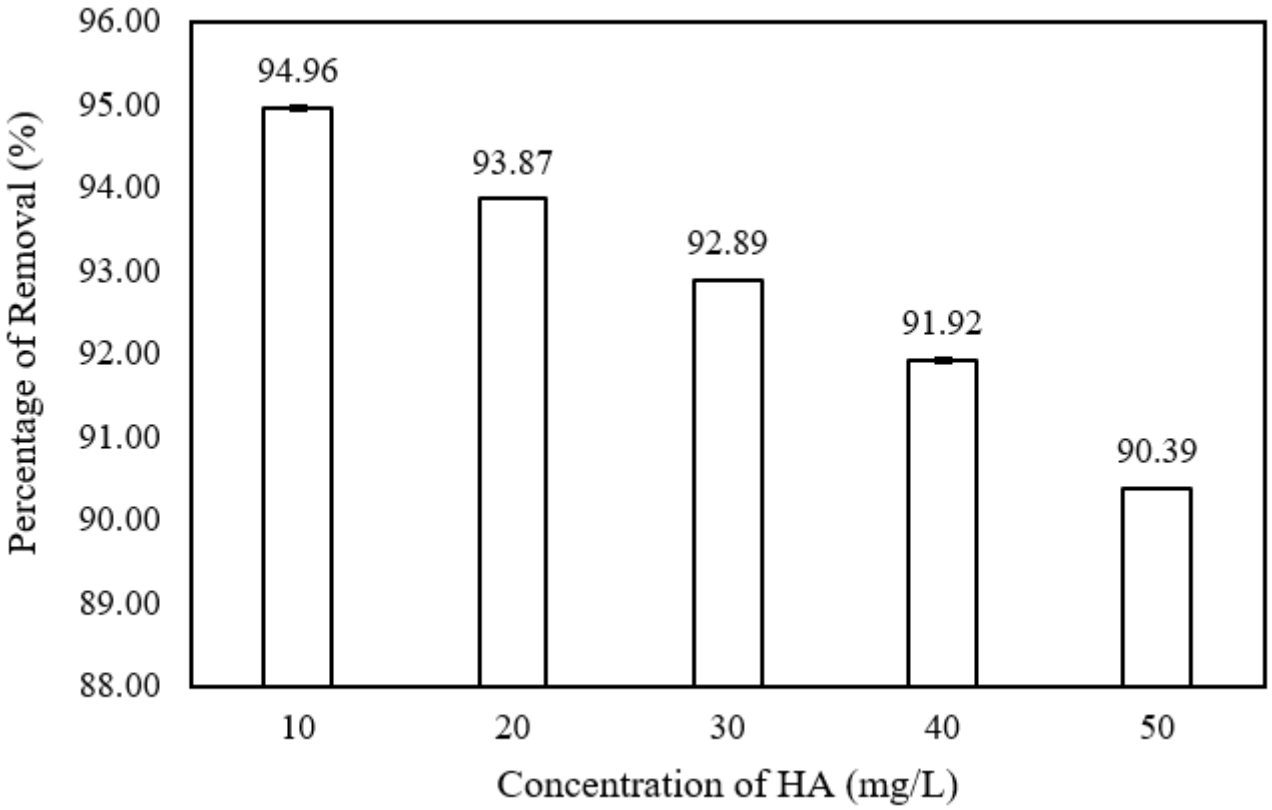

Figure 2

Percentage of Rejection (%) for different concentration of HA (mg/L)

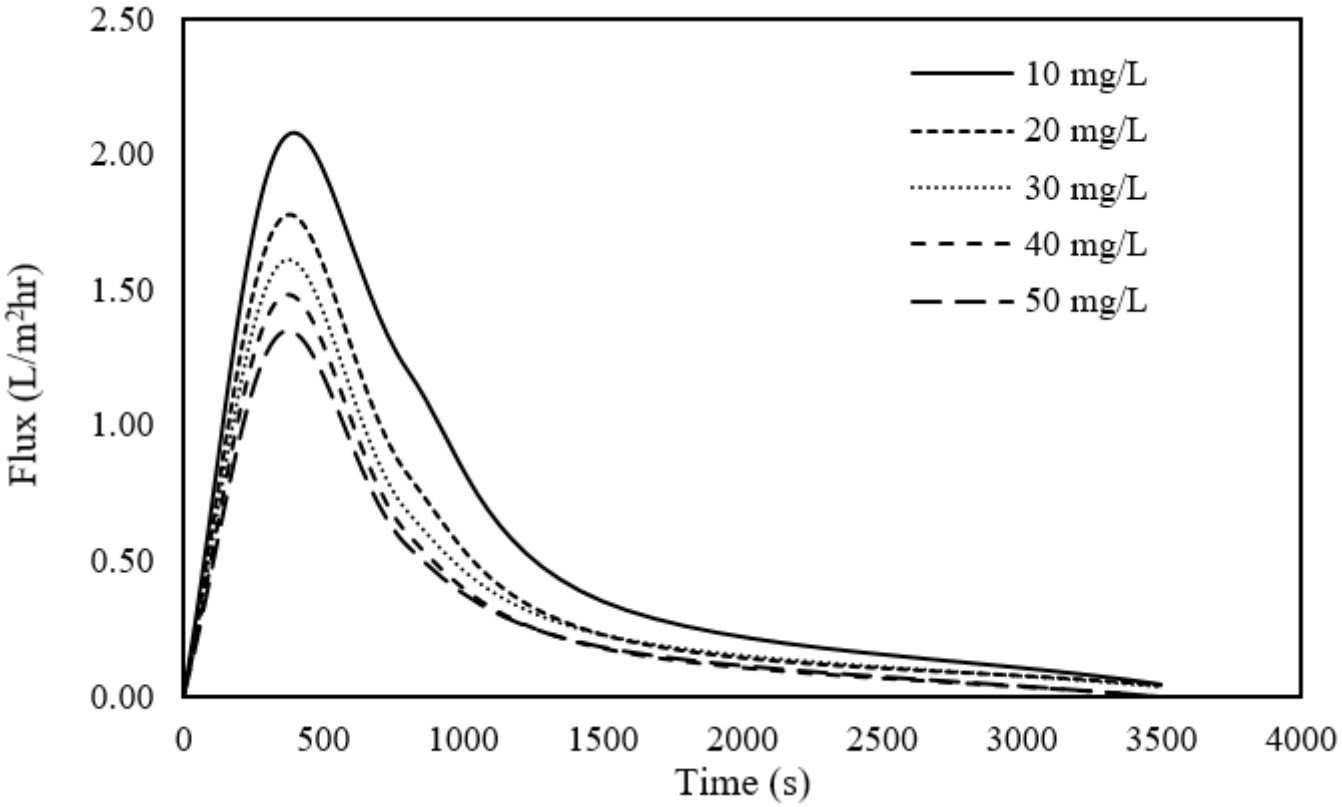

Figure 3

Filtration flux towards different concentration of HA (mg/L)

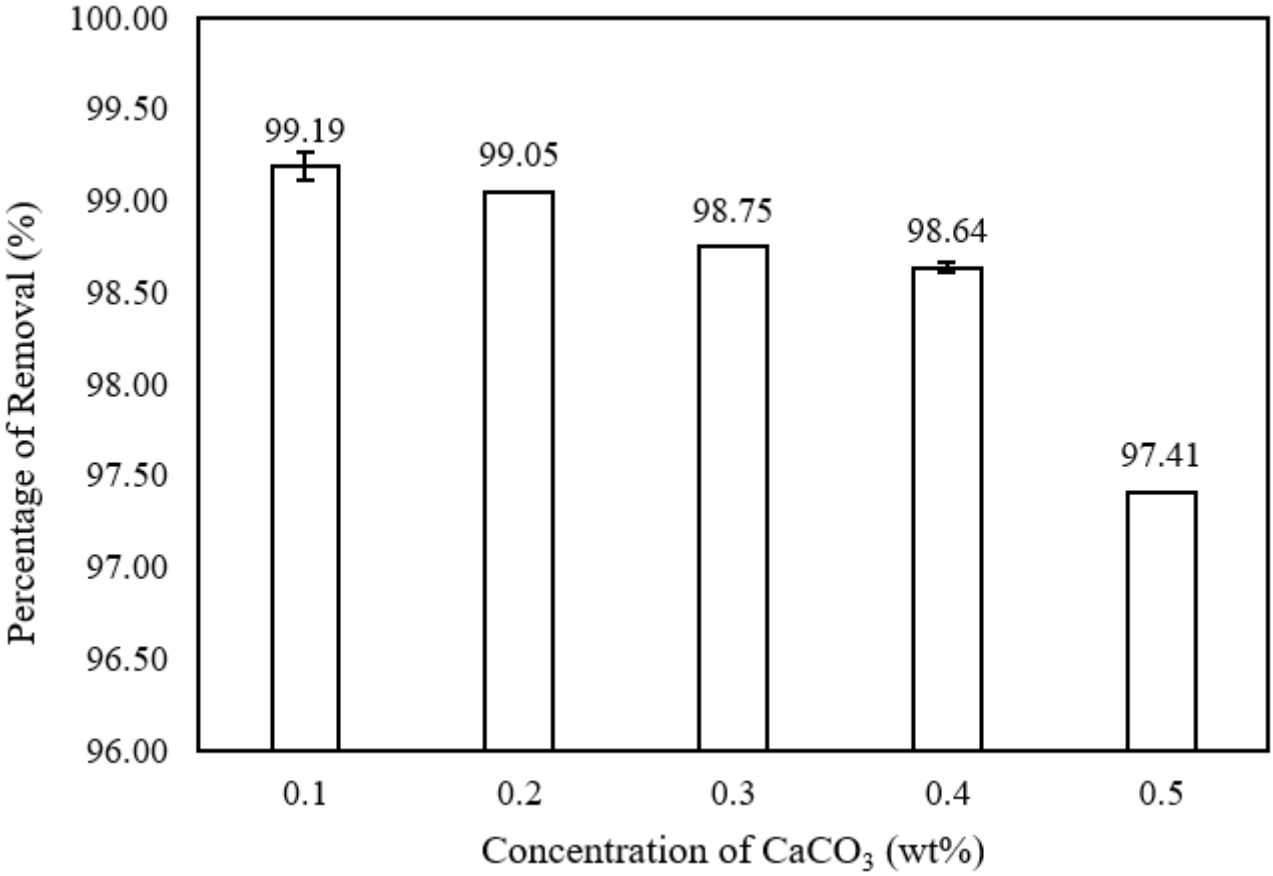

Figure 4

The rejection (%) of $CaCO_3$ as feed filtration

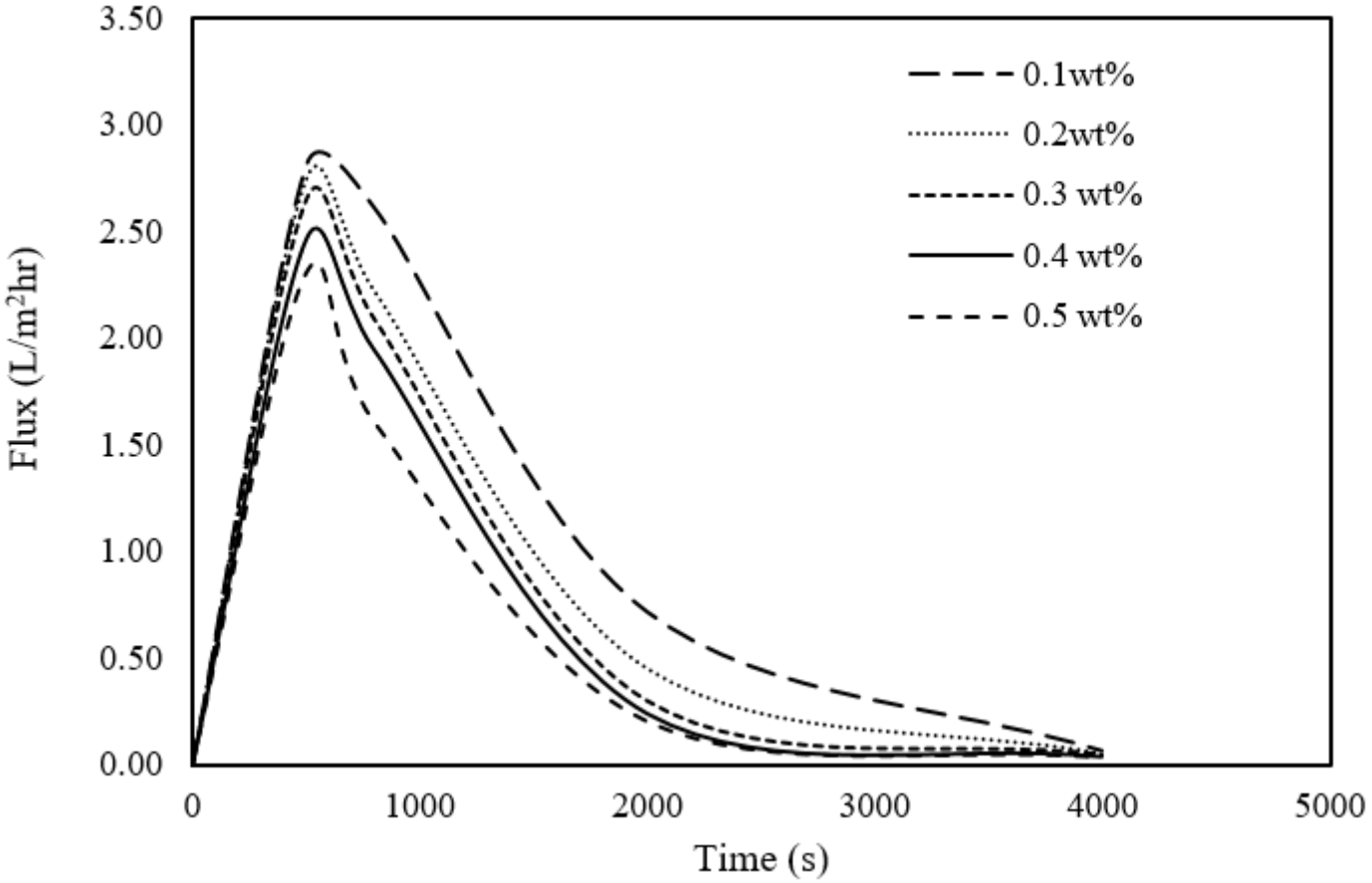

Figure 5

Flux Profile towards different $CaCO_3$ concentration

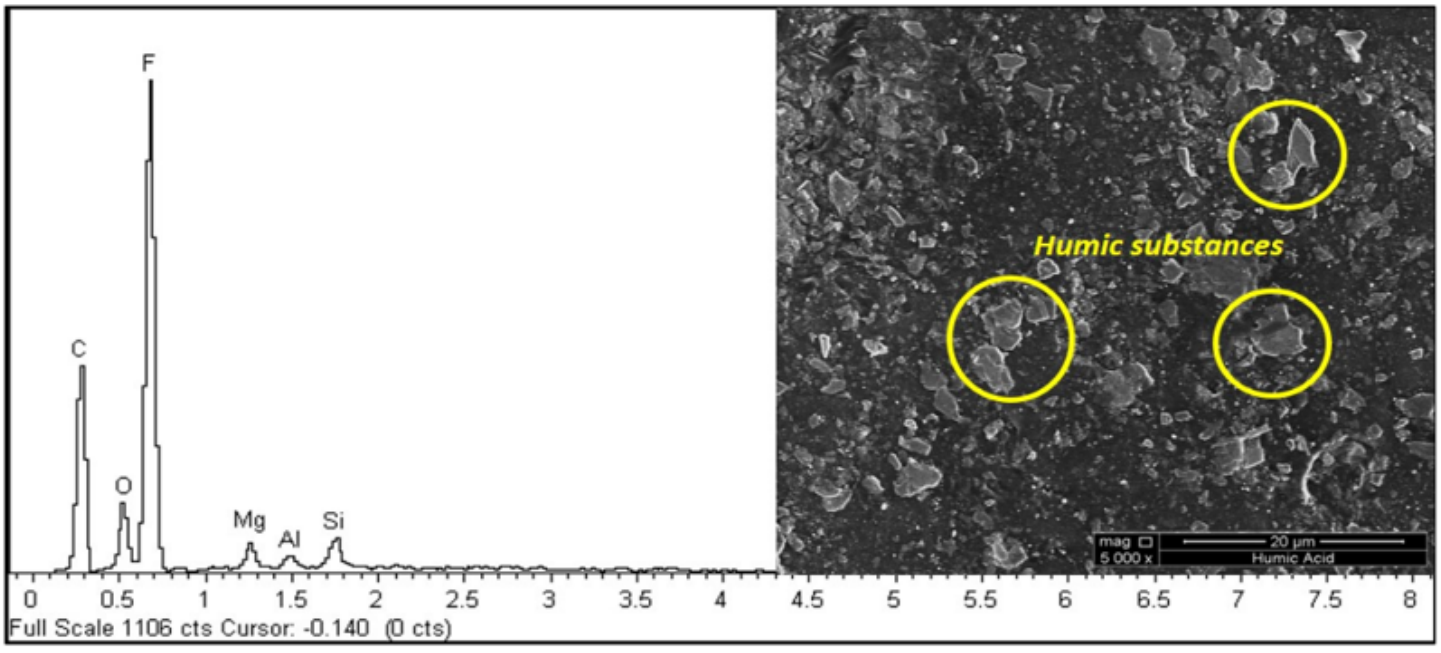

Figure 6

SEM-EDX analysis of humic substance formed on membrane surface

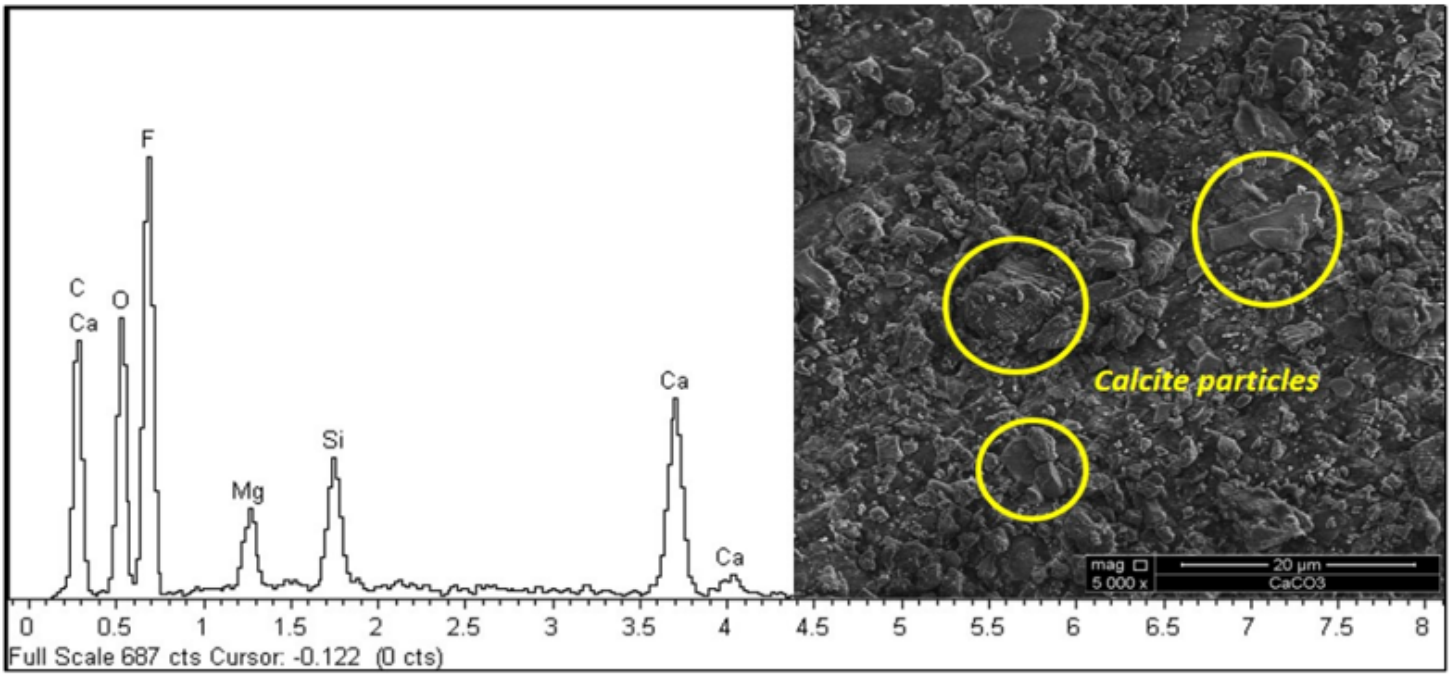

Figure 7

SEM-EDX analysis of inorganic scaling of $CaCO_3$ deposit on membrane surface

(a)

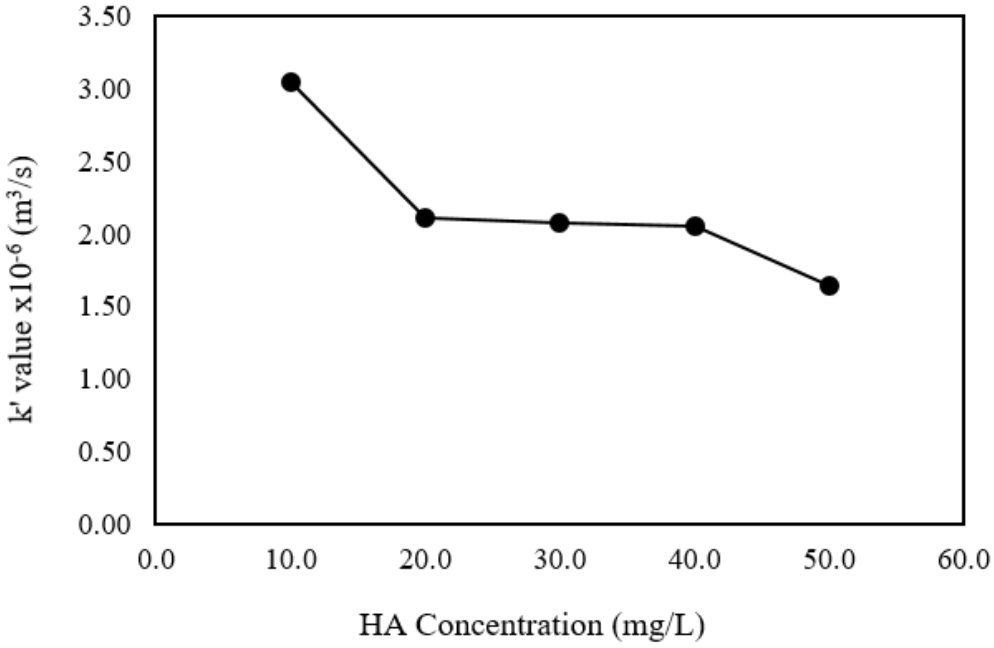

(b)

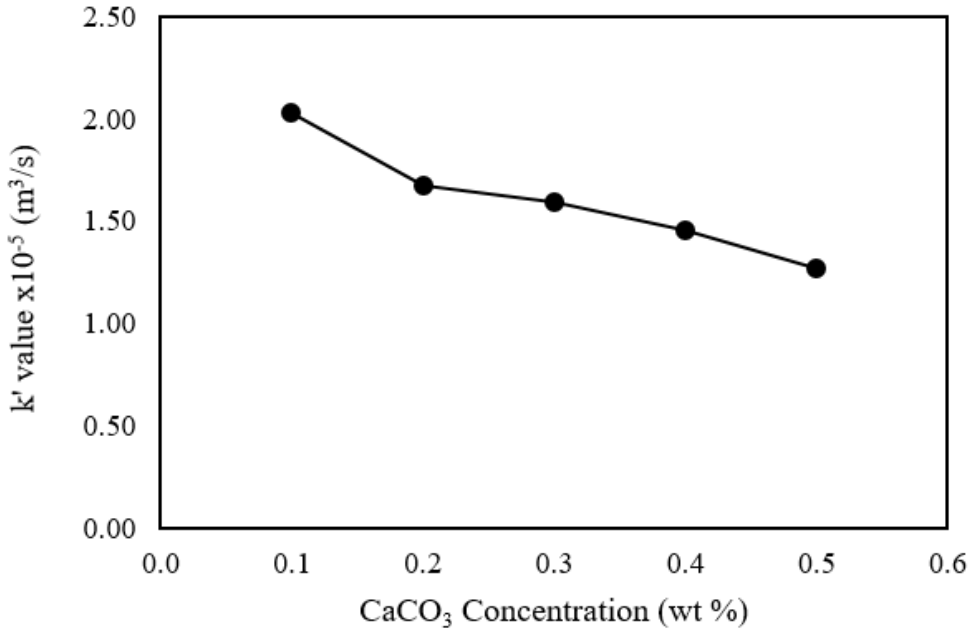

Figure 8

k' value (m^3/s) of GDU process for (a) HA and (b) $CaCO_3$

(a)

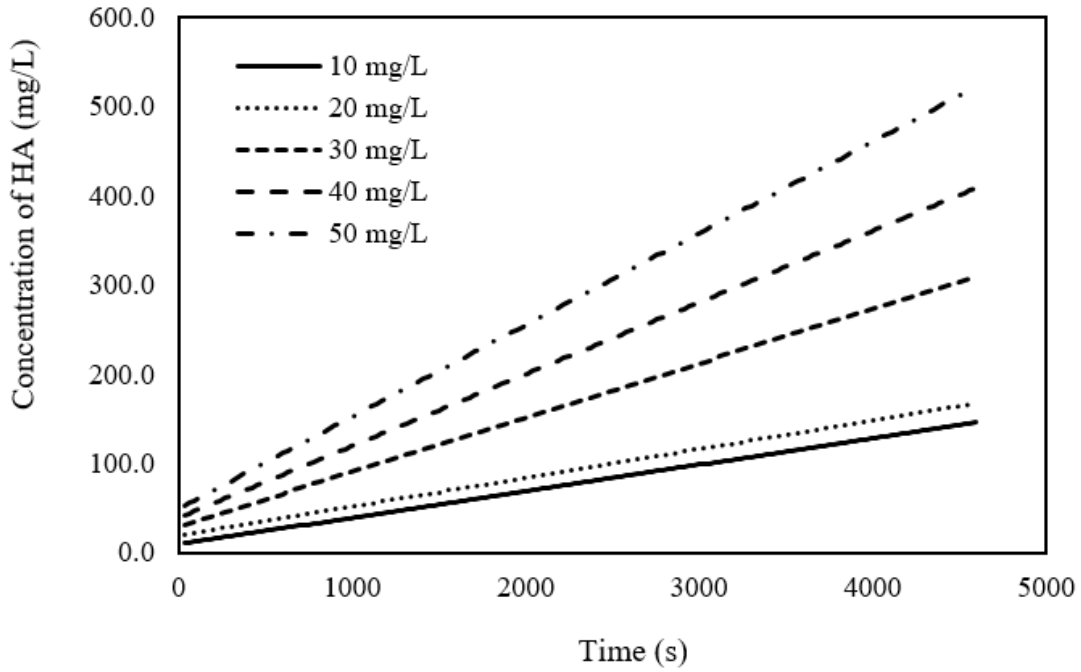

(b)

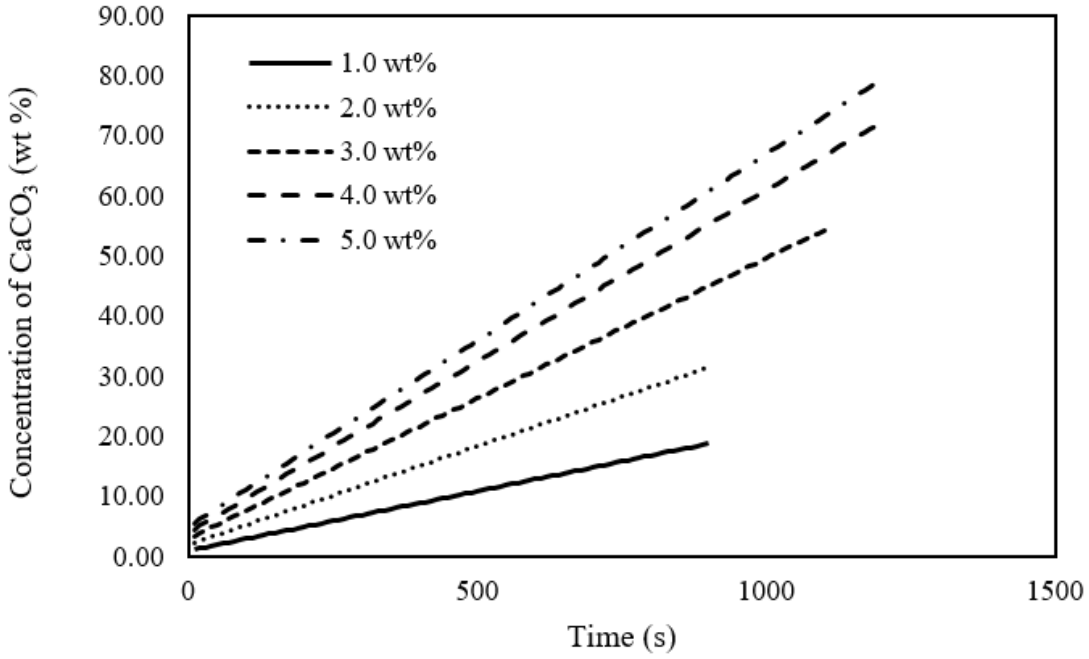

Figure 9

Concentration of (a) HA and (b) $CaCO_3$ in the retentate over the time

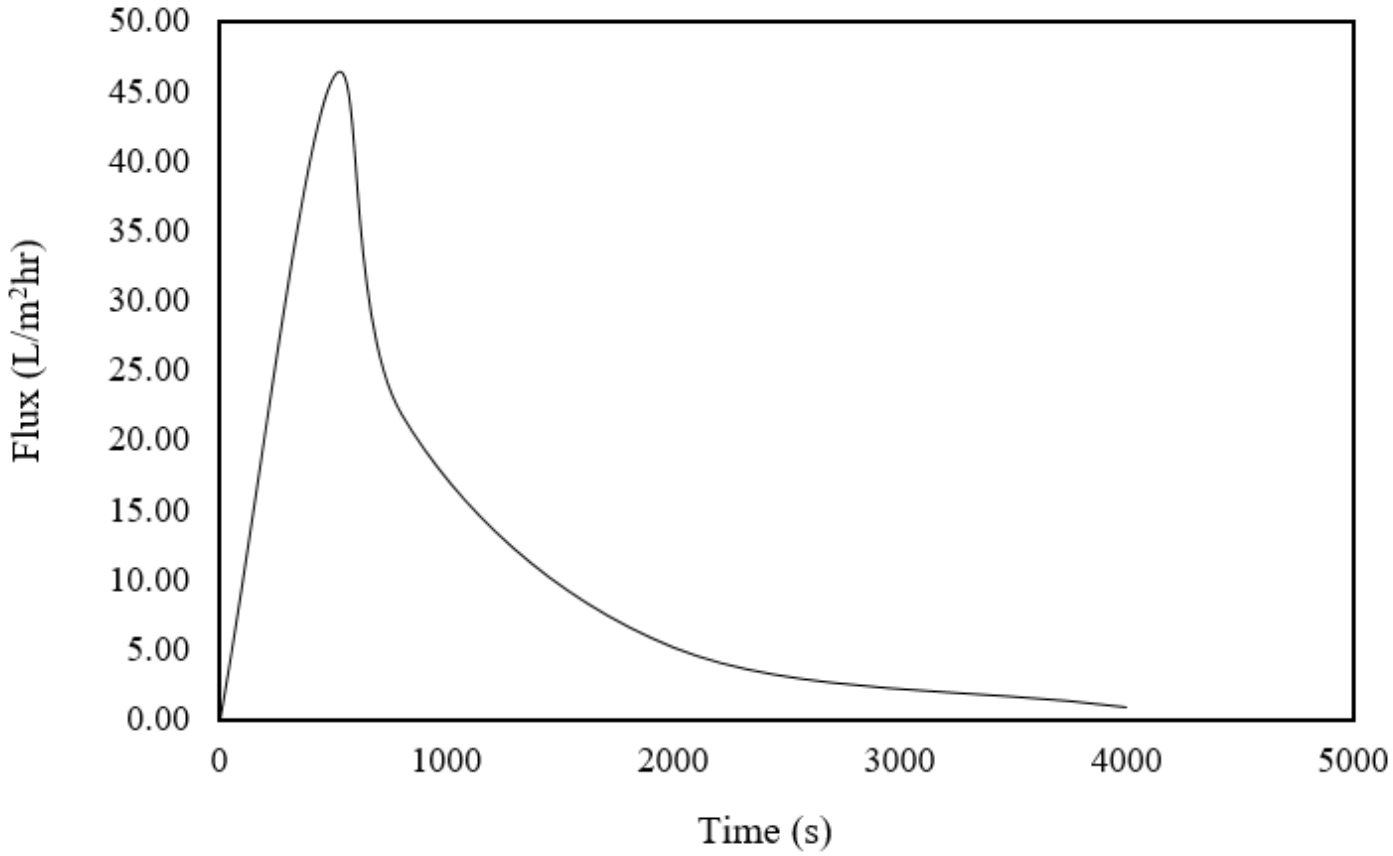

Figure 10

Filtration flux of Kerian River water samples using GDU membrane system